

## Fuzzy Clustering Based Medical Image Watermarking

Nyma Alamgir<sup>†</sup> · Jong-Myon Kim<sup>‡‡</sup>

### ABSTRACT

Medical image watermarking has received extensive attention as wide security services in the healthcare information system. This paper proposes a blind medical image watermarking approach on the segmented gray-matter (GM) images by utilizing discrete wavelet transform (DWT) and discrete cosine transform (DCT) along with enhanced suppressed fuzzy C-means (EnSFCM) for the optimal selection of sub-blocks position to insert a watermark. Experimental results show that the proposed approach outperforms other methods in terms of peak signal to noise ratio (PSNR) and M-SVD. In addition, the proposed approach shows better robustness than other methods in normalized correlation (NC) values against several attacks, such as noise addition, filtering, JPEG compression, blurring, histogram equalization, and cropping.

**Keywords :** Medical Image Watermarking, Fuzzy C-means, MRI Image, Discrete Wavelet Transform, Discrete Cosine Transform

## 퍼지클러스터링 기반 의료 영상 워터마킹

Nyma Alamgir<sup>†</sup> · 김 종 면<sup>‡‡</sup>

### 요 약

의료 영상 워터마킹은 헬스케어 정보 시스템의 보안 서비스 분야에서 많은 주목을 받고 있다. 본 논문은 워터마킹을 삽입할 최적의 서버 블록 위치 선택을 위한 개선된 퍼지 클러스터링 기법, 이산 웨이블릿 변환 및 이산 코사인 변환을 분할된 회백질 의료 영상에 적용한 블라인드 의료 영상 워터마킹 기법을 제안한다. 모의실험결과, 제안한 워터마킹 기법은 기존의 기법들보다 PSNR과 M-SVD에서 우수한 성능을 보였다. 또한, 제안한 워터마킹 기법은 노이즈 첨가, 필터링, JPEG 압축, 블러링, 히스토그램 균일화, 크로핑과 같은 공격에서도 기존의 기법들보다 정규화된 연관성 값에서 보다 강인함을 보였다.

**키워드 :** 의료 영상 워터마킹, 퍼지 클러스터링, MRI 영상, 이산 웨이블릿, 이산 코사인 변환

### 1. Introduction

With the fast advancement in information and communication technologies, new challenges have arisen in the context of easier access, manipulation and distribution of medical data in healthcare delivery and medical data management systems. At the same time, these advances come along with new threats for inappropriate use of medical information[1, 2]. The

necessity of fast and secure transmission in order to prevent unauthorized accesses is vital in the e-health environment. The typical e-diagnosis model is shown in Fig. 1, where medical images can be sent by a patient through the internet to a primary physician and the primary physician can also transfer the images to another physician. The medical images are then stored in the patient historical database for future diagnosis[3].

Security of medical information derives from strict ethics and rules that dictate three major characteristics: confidentiality, reliability, and availability. Confidentiality means that only the authorized person can access to the medical information. Reliability has two aspects: integrity and authenticity. Integrity means that the information should not be modified by any non-authorized people. Authenticity means that the information should be

\* This work was supported by the National Research Foundation of Korea(NRF) grant funded by the Korea government(MEST) (No. NRF-2013R1A2A2A05004566).

† 비회원: 울산대학교 전기공학부

‡‡ 정회원: 울산대학교 전기공학부 조교수

논문접수: 2012년 10월 30일

수정일: 1차 2013년 3월 21일

심사완료: 2013년 3월 26일

\* Corresponding Author: Jong-Myon Kim(jongmyon.kim@gmail.com)

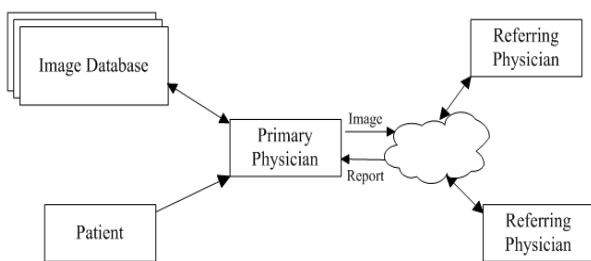


Fig. 1. Typical e-health

originated from the correct source. Availability means that entitled users have the ability to use the information in the normal condition of access[4].

There are three main applications for inserting the watermark in the medical domain: 1) data hiding to facilitate the data management, 2) security control to verify that the image is intact, and 3) authenticity to prove that the image is really what the user supposes it is [5–6]. To facilitate these applications, we have to trade off among three basic requirements: robustness, capacity, and transparency. Robustness inhibits the ability of resisting intentional or unintentional image processing operations. Capacity is the maximum amount of information that can be hidden without degrading the image quality. Transparency refers to the similarity of the watermarked image with the host image [7]. Most medical image watermarking researches have focused on developing watermarking systems that preserve image fidelity as well as robustness. In this paper, we propose a suitable tailored watermarking approach for medical images that utilizes discrete wavelet transform (DWT) and discrete cosine transform (DCT) along with enhanced suppressed fuzzy C-means (EnSFCM), which is insensitive to the fuzzy factor and yields better segmentation performance, for selecting the position of watermark, maintaining the robustness and ensuring the safety of medical data.

The rest of the paper is organized as follows. Section 2 summarizes previous related research. Section 3 describes the embedding and extracting procedure of the proposed approach. Section 4 evaluates the validity of the proposed approach, and Section 5 concludes the paper.

## 2. Related Research

Researches in the field of medical image watermarking (MIW) are categorized into three applications: 1) authentication, 2) data-hiding, and 3) combined authentication and data hiding. Authentication application

is used to identify the source of the medical image, where watermarks are located at the regions or pixels of the image. Data-hiding application is used to hide information in the image, maintaining the imperceptibility high. Depending on the purpose of the watermarking (authentication, data hiding, or both), a proper watermarking technique is chosen accordingly[8].

Chao et al. proposed a data-hiding technique called the bipolar multiple-number base to provide capabilities of authentication, integration, and confidentiality for an electronic patient record (EPR) transmitted among hospitals through the Internet[9]. The algorithm is based on substitution and permutation operations, and the confidentiality is achieved by decrypting the entire message not only with digital signatures, but also with the exact copy of the original mark image and hidden image. Zhou et al. proposed a watermarking method to verify the authenticity and integrity of digital mammography images[10]. In this method, both the digital signature and patient data are encrypted to form a digital envelope which is embedded into the least significant bits (LSBs) of randomly selected pixels of the image. In [11], a frequency domain technique based on discrete wavelet transform (DWT) with quantization methods was proposed to embed multiple watermarks for security and proper diagnosis. Acharya et al. introduced an LSB technique of embedding EPR data in medical images [4]. In this technique, text data was encrypted before interleaving with images to ensure greater security. Amirgholipour et al. proposed a combined DWT and discrete cosine transform (DCT) technique, where a scrambled logo was embedded in certain coefficient sets of 3-level DWT of host images[12]. They exploited the properties of both wavelet and cosine transform to embed watermark information in the most robust and imperceptible part of the image. In [13], the fuzzy c-means (FCM) and DCT-based watermarking approach was proposed. This approach achieved imperceptibility and robustness by detecting suitable DCT blocks in which watermarks were embedded. However, it works on a particular modality of medical images.

To enhance the performance of medical image watermarking, we propose a hybrid approach that incorporates DWT and DCT along with FCM for the optimal selection of position to insert a watermark. Experimental results show that the proposed approach achieves high PSNR (about 43dB) and low M-SVD value (about 17). In addition, we compare normalized correlation (NC) values of the proposed approach and other methods

to evaluate the robustness against several attacks including noise addition, filtering, JPEG compression, blurring, histogram equalization, and cropping.

### 3. The Proposed Medical Image Watermarking Approach

#### 3.1 Watermark Embedding Procedure

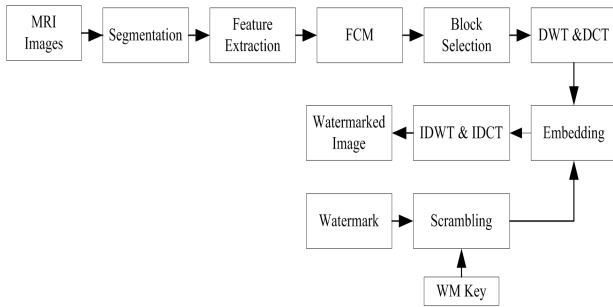


Fig. 2. Proposed watermark embedding procedure

Fig. 2 show the proposed watermark embedding procedure. The original MRI images are segmented into three different classes including Gray Matter (GM), White Matter (WM) and Cerebra-Spinal Fluid (CSF) by using an Enhanced Suppressed Fuzzy C-Means (EnSFCM) algorithm[14] which is insensitive to the fuzzy factor and yields better segmentation performance. SFCM gives the highest priority to the biggest membership and suppresses the others. It modifies the membership function using following equations

$$\begin{aligned} \mu_{pk} &= 1 - \alpha \sum_{i \neq p} \mu_{ik} = 1 - \alpha + \alpha \mu_{pk} \\ \mu_{pk} &= \alpha \mu_{pk}, \quad i \neq p \end{aligned} \quad (1)$$

where  $\mu_{pk}$  implies that data point  $x_k$  belongs to the largest cluster  $p$  and  $\alpha$  is a suppression factor with a range of  $[0, 1]$ . When  $\alpha = 0$ , the algorithm is equal to the hard c-means (HCM) clustering algorithm; and when  $\alpha = 1$ , the algorithm becomes FCM algorithm. So, SFCM establishes reasonable relationship between HCM and FCM clustering algorithm.

In order to embed the watermark, GM images are selected because the act of introspection links to the anatomy of the gray matter of our brain. In addition, GM images represent high signal intensity and good textural properties[15]. Firstly GM images are divided into  $8 \times 8$  blocks. To increase the perceptual imperceptibility, we utilize FCM to choose the position for watermark

embedding. To build a data set for FCM, we calculate the energy, contrast and entropy from each block. Cluster centroids and lower membership values are used for choosing suitable blocks for watermark embedding. Steps of the embedding process are given below:

Step 1: The original image is segmented by using EnSFCM and then GM image is taken as a cover image for concealing watermark.

Step 2: The GM cover image is divided into  $8 \times 8$  blocks, and we calculate energy, contrast and entropy of each block. We then build the dataset  $P = \{\text{Energy, Contrast, and Entropy}\}$  as an input of FCM.

Step 3: Suitable blocks are chosen based on the membership value of FCM to embed a watermark.

Step 4: Selected blocks are transformed into frequency sub-bands by using 2-level DWT. HH1 band is then selected because the higher sub-band has better concealing effect for embedding watermark.

Step 5: DCT is applied to each HH1 sub-band and then the mid-frequency coefficients are extracted from the transformed blocks.

Step 6: The watermark text image is scrambled with an Arnold algorithm for  $k_1$  times and then the scrambled watermark is obtained. Scrambled times  $k_1$  are used as the secret key.

Step 7: Two uncorrelated pseudorandom sequences are generated in which one sequence is used to embed the watermark bit 0 ( $pn_0$ ) and the other one for watermark bit 1 ( $pn_1$ ). The scrambled watermark is embedded in the mid-frequency DCT coefficients. Let  $X$  is the mid-frequency coefficients of the DCT transformed block, and then the embedding is done as follows:

$$X' = \begin{cases} X + \alpha^* pn_0 \\ X + \alpha^* pn_1 \end{cases} \quad (2)$$

Step 8: Inverse DCT (IDCT) is applied to each block after coefficients have been modified. Then, these modified blocks are converted back to the spatial domain by performing 2-level IDWT and the watermarked GM image is found. The linear combination of watermarked GM image with WM and CSF image is finally performed in order to get the final watermarked image.

A brief introduction for DCT, DWT, and FCM is given below.

#### 1) Discrete Wavelet Transform

Discrete Wavelet transform (DWT) is a technique that decomposes an image into low, middle, and high

frequency bands by applying a 2-dimensional filter. It provides both frequency and spatial description of an image[16]. The anisotropic properties of human visual system (HVS) can be presented by using DWT. The filters divide the image into four non-overlapping multi-resolution coefficient sets, such as a lower resolution approximation image (LL1) with horizontal (HL1), vertical (LH1) and diagonal (HH1) detail components. It represents two types of coefficient sets in which LL1 sub-band represents the coarse level coefficients, while other three sub-bands present the finest scale wavelet coefficients. The spatial-frequency localization properties of the wavelet transform is better than those of discrete Fourier transform (DFT) and DCT (DCT) to exploit the masking effect of HVS [7]. For this reason, we manipulate DWT to choose a proper sub-band in terms of robustness and imperceptibility.

## 2) Discrete Cosine Transform

Discrete Cosine Transform (DCT) is a technique that converts a signal into elementary frequency components [17]. The transformed matrix consists of AC and DC coefficients. In the DCT transformed block, the top left corner element is called a DC coefficient that is perceptually significant, and the remaining coefficients are AC coefficients that are perceptually insignificant. In order to obtain the frequency components of an image, these coefficients are zig-zag scanned in decreasing order and computed as follows:

$$y(u,v) = \sqrt{\frac{2}{M}} \sqrt{\frac{2}{N}} \alpha_m \alpha_n \cdot \sum_{x=0}^{M-1} \sum_{y=0}^{N-1} \left\{ x(m,n) \times \cos \frac{(2m+1)\mu\pi}{2M} \cos \frac{(2n+1)\mu\pi}{2N} \right\} \quad (3)$$

where  $x$  is the input image having  $N \times M$  pixels,  $x(m, n)$  is the intensity of the pixel in row  $m$  and column  $n$  of the image and  $y(u, v)$  is the DCT coefficients in row  $u$  and column  $v$  of the DCT matrix. In addition,  $\alpha_m$  and  $\alpha_n$  are calculated as follows:

$$\alpha_m = \begin{cases} \frac{1}{\sqrt{2}} & m = 0 \\ 1 & m = 1, 2, \dots, M-1 \end{cases} \quad (4)$$

$$\alpha_n = \begin{cases} \frac{1}{\sqrt{2}} & n = 0 \\ 1 & n = 1, 2, \dots, N-1 \end{cases}$$

The image is reconstructed by applying an inverse DCT as follows:

$$x(m,n) = \sqrt{\frac{2}{M}} \sqrt{\frac{2}{N}} \sum_{u=0}^{M-1} \sum_{v=0}^{N-1} \left\{ a_m \alpha_n y(u,v) \times \cos \frac{(2m+1)\mu\pi}{2M} \cos \frac{(2n+1)\mu\pi}{2N} \right\} \quad (5)$$

## 3) Fuzzy C-Mean Clustering

Fuzzy C-means (FCM) is a data clustering algorithm in which data can belong to several groups based on the membership value. This algorithm is one of the most prominent clustering techniques for image segmentation, feature extraction, and pattern recognition[18].

Let  $X=\{x_1, x_2, x_3, \dots, x_n\}$ , where  $n$  is the number of image pixels. The conventional FCM algorithm sorts the data set  $X$  into  $c$  classes. The standard FCM objective function is defined as follows:

$$J_m(U, V) = \sum_{i=1}^c \sum_{k=1}^n \mu_{ik}^m d^2(x_k, v_i) \quad (6)$$

where  $d(x_k, v_i)$  is the Euclidian distance between the data point  $x_k$  and the centroid  $v_i$  of the  $i$ th class, and  $\mu_{ik}^m$  is the degree of membership of the data  $x_k$  to the  $k^{\text{th}}$  class. The parameter  $m$  which is called the fuzzy factor controls the fuzziness of the resulting partition, ( $m \geq 1$ ), and  $c$  is the total number of classes. FCM is an iterative algorithm that produces an optimal number of  $c$  classes by minimizing the objective function  $J_m(U, V)$  with updated values of  $\mu_{ik}$  and  $v_i$  according to the following equations:

$$\mu_{ik} = \left[ \sum_{j=1}^c \left( \frac{d^2(x_k, v_j)}{d^2(x_k, v_i)} \right)^{\frac{1}{m-1}} \right]^{-1} \quad (7)$$

$$v_i = \frac{\sum_{k=1}^n \mu_{ik}^m \cdot x_k}{\sum_{k=1}^n \mu_{ik}^m} \quad (8)$$

As  $J_m$  is iteratively minimized,  $v_i$  becomes more stable. The pixel clustering iterations are terminated when the termination measurement  $\max_{1 \leq i \leq c} \{ \| v_i^{(t)} - v_i^{(t-1)} \| \} < \epsilon$  is satisfied, where  $v_i^{(t)}$  are the new centroids for  $1 \leq i \leq c$ ,  $v_i^{(t-1)}$  are the previous centroids for  $1 \leq i \leq c$ , and  $\epsilon$  is a predefined termination threshold. The output of the FCM algorithm is the cluster centroids  $V$  and the fuzzy partition matrix  $U_{CxN}$ .

## 3.2 Watermark Extracting Procedure

Fig. 3 illustrates the proposed watermark extraction

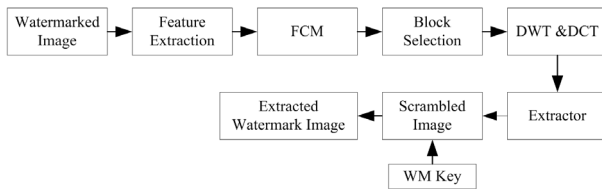


Fig. 3. Proposed watermark extraction procedure

process which performs the blind extraction of the watermark.

Step 1: The watermarked image is divided into  $8 \times 8$  blocks and the dataset of FCM is built.

Step 2: FCM is applied to find the blocks corresponding to the membership values in which watermarks are embedded.

Step 3: The selected blocks is decomposed by using 2-level DWT and then HH1 is further transformed by DCT in order to extract the watermark.

Step 4: We extract the mid-frequency coefficients of each DCT block and calculate the correlation between the mid-frequency coefficients and the pseudorandom sequences of  $pn0$  and  $pn1$ . If the correlation with the  $pn0$  is higher than that with  $pn1$ , the extracted bit is then considered as 0, otherwise the extracted bit is considered as 1.

Step 5: We reconstruct the scrambled watermark using the extracted bits and then recover the watermark with an Arnold transform using  $k1$ .

#### 4. Experimental Results and Analysis

Four different types of T1 weighted MRI images ( $256 \times 256$ ) with a gray level 'ITC' text ( $32 \times 32$ ) as a watermark are used in this study. In addition, we use the gain factor,  $\alpha = 55$ . The performance of the proposed approach is compared with the following existing methods:

Method 1: DWT-DCT based algorithm[12].

Method 2: FCM-DCT based algorithm[13].

##### 4.1 HVS based Evaluation

Imperceptibility is measured by peak signal-to-noise ratio (PSNR) which determines the distortion level in the original image due to the watermark insertion. PSNR is defined as a ratio of maximum possible power of a signal with the power of noise that affects the fidelity of the representation. It is defined as:

$$\begin{aligned} PSNR &= 10 \log_{10} \left( \frac{MAX_1^2}{MSE} \right) \\ &= 20 \log_{10} \left( \frac{MAX_1}{MSE} \right) \end{aligned} \quad (9)$$

where  $MAX_1$  is the maximum possible pixel value of the image. Mean squared error (MSE) for two  $m \times n$  monochrome images is defined by the following:

$$MSE = \frac{1}{mn} \sum_{i=0}^{m-1} \sum_{j=0}^{n-1} [I(i,j) - K(i,j)]^2 \quad (10)$$

Furthermore, M-SVD is used to numerically express the quality of the distorted images. M-SVD measures the distance between the singular values of the host image block and the singular values of the distorted image block.

$$M-SVD = \frac{\sum_{i=1}^{(k/n) \times (k/n)} |D_i - D_{mid}|}{(k/n) \times (k/n)} \quad (11)$$

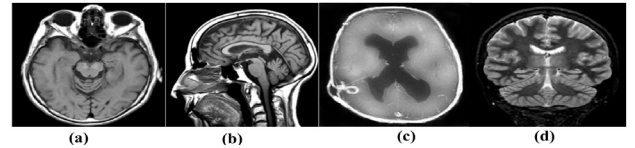


Fig. 4. Original cover images



Fig. 5. Watermarked GM images

where  $k \times k$  is the image size.  $D_i$  is the distance between original block and distorted block, and  $D_{mid}$  represents the midpoint of the sorted  $D_i$ . Lower M-SVD values mean that the watermarked image is less distorted by watermark insertion. Fig. 4 and Fig. 5 show the original cover images and watermarked GM images using the proposed approach, respectively. In addition, Fig. 6 shows PSNR and M-SVD values of watermark images using the proposed and conventional approaches. The proposed approach outperforms other methods in terms of PSNR and M-SVD, where high PSNR and low M-SVD are better [19].

##### 4.2 Robustness to Various Attack

In addition, we evaluate the robustness of the proposed

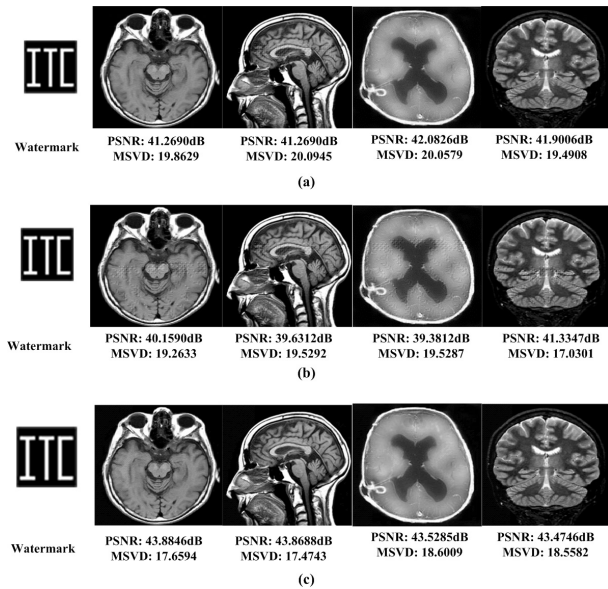


Fig. 6. Quality evaluation of the watermarked images with PSNR and M-SVD values using (a) Method 1, (b) Method 2, and (c) proposed approach

approach against various attacks including noise addition, filtering, histogram equalization, blurring, cropping and JPEG compression. We use the normalized correlation (NC) value to identify the similarity between the original and extracted watermark. If the calculated NC is 1, the original and watermarked images are exactly the same. NC value is measured by the following equation:

$$NC = \frac{\sum_{i=0}^{M-1} \sum_{j=0}^{N-1} w(i,j) \times w^*(i,j)}{\sum_{i=0}^{M-1} \sum_{j=0}^{N-1} [w(i,j)]^2} \quad (12)$$

where  $M \times N$  is the watermark image size,  $w(i, j)$  is the intensity value of the original watermark, and  $w^*(i, j)$  is the intensity value of the extracted watermark image. Table 1 presents NC values of the extracted watermark using the proposed approach and those using other conventional methods after applying various attacks. The proposed approach achieves considerably higher NC values than those of others.

In addition to quantitative evaluation, qualitative evaluation is also important. Fig. 7 shows resulting watermarked images and extracted watermark using the proposed and other conventional approaches after applying various attacks. In case of median filtering, each pixel is modified by median values which may cause distorted watermark. With cropping attack, we lose some information, resulting in distorting watermark.

## 5. Conclusion

Digital watermarking has the potential to provide security to health informatics. In this paper, we proposed a robust medical image watermarking system that

Table 1. NC values of the extracted watermark using three different watermark algorithms

Attacks	Approach 1					Approach 2				Proposed		Algorithm	
	Fig 4a	Fig 4b	Fig 4c	Fig 4d	Fig 4a	Fig 4b	Fig 4c	Fig 4d	Fig 4a	Fig 4b	Fig 4c	Fig 4d	
<b>GN</b>	0.8220	0.7713	0.7750	0.7556	0.8711	0.7806	0.7916	0.9086	0.9949	1	0.9949	1	
<b>SPN</b>	0.9606	0.9174	0.8664	0.9432	0.9771	0.9320	0.9616	0.9690	0.9920	0.9798	0.9798	0.9747	
<b>GF</b>	0.9562	0.9687	0.9124	0.9011	0.9894	0.9634	0.9947	0.9988	0.9848	0.9949	0.9949	1	
<b>MDF</b>	0.4789	0.3967	0.3899	0.4234	0.8304	0.6968	0.8135	0.8761	0.8434	0.8790	0.9192	0.8990	
<b>MF</b>	0.8374	0.6848	0.8392	0.8612	0.8515	0.7080	0.8485	0.8950	0.9798	0.9747	0.9192	0.9849	
<b>ADF</b>	0.9374	0.9168	0.8937	0.9091	0.9647	0.8642	0.9317	0.9959	0.9899	0.9897	0.9646	1	
<b>JPEG</b>	0.9957	0.9827	0.9644	0.9831	0.9548	0.9823	0.9994	0.9747	1	1	0.9848	1	
<b>Blur</b>	0.9285	0.9437	0.9263	0.9377	0.9239	0.8710	0.9261	0.9603	0.9747	0.9646	0.9697	0.9899	
<b>Crop</b>	0.5759	0.4160	0.6067	0.6440	0.8159	0.7743	0.7828	0.8850	0.8515	0.7902	0.7835	0.8993	
<b>HE</b>	0.9399	0.9119	0.9349	0.9623	0.9236	0.8971	0.9556	0.9637	0.9949	1	1	1	

**GN:** Gaussian Noise with zero mean and 0.01 variance. **SPN:** Salt & Pepper Noise with density of 0.1. **GF:** Gaussian low-pass filtering of 3×3window. **MDF:** Median Filtering of 2×2window. **MF:** Mean Filtering. **ADF:** Adaptive Filtering (wiener of 3×3window). **JPEG:** JPEG Compression. **Blur:** Blurring Effect with zero mean and 0.001 variance. **Crop:** Cropping of 12%. **HE:** Histogram Equalizing.

Attack	Attacked Image	Method 1	Method 2	Proposed	Attack	Attacked Image	Method 1	Method 2	Proposed
GN					ADF				
SPN					JPEG				
GF					Blur				
MDF					Crop				
MF					HE				

Fig. 7. Watermarked images and extracted watermark using the proposed and other conventional approaches

incorporates DWT and DCT along with FCM for the optimal selection of the position to insert a watermark. The watermark was embedded into the segmented GM images and the final watermarked image was then formed by the linear combination of the watermarked GM image with the other segmented images. The proposed approach achieves higher PSNR and lower M-SVD values than other conventional methods. In addition, the proposed approach outperforms other conventional methods in terms of NC values after applying various attacks, such as including noise addition, filtering, histogram equalization, blurring, cropping and JPEG compression.

## Reference

- [1] A. Giakoumaki, S. Pavlopoulos, D. Koutsouris, "Multiple Watermarking applied to Health Information Management," IEEE Transactions on Information Technology in Biomedicine, Vol.10, No.4, pp.722–732, 2006.
- [2] F. Y. Shih, and Y.-T. Wu, "Robust Watermarking and Compression for Medical Images based on Genetic Algorithms," International Journal of Information Sciences, Vol.175, No.3, pp.200–216, 2005.
- [3] M. Lia, R. Poovendrana, and S. Narayananb, "Protecting Patient Privacy against Unauthorized Release of Medical Images in a Group Communication Environment," International Journal of Computerized Medical Imaging and Graphics, Vol.29, No.5, pp.367–383, 2005.
- [4] R. Acharya U.P. S. Bhatb, S. Kumar, and L. C. Mina, "Transmission and Storage of Medical Images with Patient Information," International Journal of Computers in Biology and Medicine, Vol.33, No.4, pp.303–310, 2002.
- [5] G. Coatrieux, L. Lecornu, B.Sankur, Ch. Roux, "A Review of Image Watermarking Applications in Healthcare," in 28th Annual International Conference of the IEEE Engineering in Medicine and Biology Society, Vol.8, pp.4691–4694, 2006.
- [6] G. Coatrieux, H. Maitre, B. Sankur, Y. Rolland, and R. Collorec, "Relevance of Watermarking in Medical Imaging," in IEEE EMBS International Conference on Information Technology Applications in Biomedicine, pp.250–255, 2000.
- [7] V.S. Jabade and S.R. Gengaje, "Literature Review of Wavelet Based Digital Image Watermarking Techniques," International Journal of Computer Applications, Vol.31, No.1, pp.28–35, 2011.
- [8] O.M. Al-Qershi and B.E. Khoo, "ROI-based Tamper Detection and Recovery for Medical Images using Reversible Watermarking Technique," in IEEE International Conference on Information Theory and Information Security (ICITIS), pp.151–155, 2010.
- [9] H. M. Chao, C. M. Hsu, and S. G. Miaou, "A Data-Hiding Technique with Authentication, Integration, and Confidentiality for Electronic Patient Records," IEEE Transaction on Information Technology on Biomedicine,

- Vol.6, No.1, pp.46–53, 2002.
- [10] X. Q. Zhou, H. K. Huang, and S. L. Lou, “Authenticity and Integrity of Digital Mammography Images,” IEEE Transaction on Medical Imaging, Vol.20, No.8, pp.784–791, 2001.
- [11] A. Giakoumaki, S. Pavlopoulos, and D. Koutsouris, “A Medical Image Watermarking Scheme based on Wavelet Transform,” in Proceedings of the 25th Annual International Conference of the IEEE EMBS, pp.856–859, 2003.
- [12] S. Amirgholipour and A.R. Naghsh-Nilchi, “Robust Digital Image Watermarking Based on Joint DWT-DCT,” International Journal on Digital Content Technology and its Applications, Vol.3, No.2, pp.3531–3546, 2009.
- [13] J. Wu and J. Xie, “Adaptive Image Watermarking Scheme based on HVS and Fuzzy Clustering Theory,” in International Conference on Neural Networks and Signal Processing, Vol.2, pp.1493–1496, 2003.
- [14] N. ALamgir, M. Kang, Y. K. Kwon, C. H. Kim, and J. M. Kim, “A Hybrid Technique for Medical Image Segmentation,” Journal of Biomedicine and Biotechnology, vol. 2012, Article ID 830252, 7 pages, 2012.
- [15] B. Ganeshan, K. A. Miles, R.C. Young, C. R. Chatwin, H. M. D. Gurling, and H. D. Critchley, “Three-Dimensional Textural Analysis of Brain Images Reveals Distributed Gray-Matter Abnormalities in Schizophrenia,” Eur Radiol, pp.941–949, 2010.
- [16] M. J. Shensa, “The Discrete Wavelet Transform: Wedding the Trous and Mallat Algorithms,” IEEE Trans. Signal Processing, Vol.40, No.10, pp.2464–2482, 1993.
- [17] G. Strang, “The Discrete Cosine Transform,” J. Acoustical Society of America, Vol.41, No.1, pp.135–147, 1999.
- [18] J. C. Bezdek, J. Keller, R. Krisnapuram, and N. Pal, “Fuzzy Models and Algorithms for Pattern Recognition and Image Processing,” Springer, 2005.
- [19] S. Voloshynovskiy, S. Pereira, T. Pun, J.J. Eggers, and J.K. Su, “Attacks and Benchmarking,” IEEE Communication Magazine, Vol.39, No.8, 11 pages, 2001.



Nyma Alamgir

e-mail : nymaeee@gmail.com

She received an MS degree in Electronics Engineering from University of Ulsan in 2013. Her research interests are in the area of Medical Image Processing, Multimedia Watermarking, and Image Processing.



Jong-Myon Kim

e-mail : jongmyon.kim@gmail.com

He received a PhD in electrical and computer engineering from the Georgia Institute of Technology, Atlanta, USA, in 2005. He is an Assistant Professor of Electrical Engineering at the University of Ulsan, South Korea. His research interests include many-core architecture, multimedia processing, parallel processing, and embedded systems.